Third-order Nonlinear Optical Properties of Copper(II)bis{2-[(4-iodophenyl)iminomethyl]-6-methoxy-phenolate}

Halime G. Yaglioglu[a], Asli Karakaş[b], Hseyin Ünver[c], and Ayhan Elmali[a]

[a] Ankara University, Faculty of Engineering, Department of Engineering Physics, TR-06100, Tandoğan, Ankara, Turkey
[b] Selçuk University, Faculty of Arts and Sciences, Department of Physics, TR-42049 Campus, Konya, Turkey
[c] Ankara University, Faculty of Sciences, Department of Physics, TR-06100 Tandoğan, Ankara, Turkey

Reprint requests to Prof. Ayhan Elmali. E-mail: elmali@eng.ankara.edu.tr

Z. Naturforsch. **61b,** 1355 – 1360 (2006); received April 24, 2006

Copper(II)bis{2-[(4-iodophenyl)iminomethyl]-6-methoxy-phenolate} has been synthesized, characterized by UV-visible spectroscopy, and its crystal structure determined by X-ray diffraction. The Cu atom is situated on a twofold axis and the geometry around the metal centre can be described as distorted square planar with a *trans* configuration. The absorption maxima are shorter than 450 nm, giving rise to good optical transparency in the visible and near IR. To reveal the microscopic third-order NLO properties, the static second hyperpolarizabilities have been evaluated by using the *ab initio* time-dependent Hartree-Fock (TDHF) method. According to the results, the title complex exhibits non-zero γ values, implying microscopic third-order NLO behavior.

Key words: Copper(II) Complex, Time-Dependent Hartree-Fock, Static Third-Order Hyperpolarizability, UV-visible Spectroscopy, *ab initio* Calculation

Introduction

In the last decades, NLO has become a key field in the area of photonics and optoelectronics [1 – 4]. Along with linear and quadratic effects there has been growing interest in third-order optical nonlinearity. Organic molecules have been intensively studied with respect to their potential applications as NLO media [5 – 7]. These compounds are significant third-order NLO materials. Third order materials have many important applications such as optical limiting [8], design of logic gates [9] and optical switching [10]. Metal complexes like organic compounds have several advantages as far as their third-order NLO properties are concerned. Organic substituents and transition metal ions with unfilled *d*-shells influence the nonlinearity through the interaction between the electrons in the substituents and the electrons in the main organic system [11]. Most NLO chromophores have been found in organic molecules such as stilbene [12], thiophene [13], or polyene families [14], but the introduction of a metal center as a donor or acceptor subunit has also led to various molecules with large NLO responses. Compared to organic compounds, organometallic complexes offer a larger variety of structures, the possibility of high environmental stability, and a diversity of electronic properties by virtue of the metal center. Besides, organometallic complexes possess strong metal-to-ligand charge-transfer (MLCT) transitions in the UV-visible region, or possess low-lying intervalence charge-transfer (CT) transitions. Therefore, they can effectively behave as donors and/or acceptors or as constituents of the polarizable bridge. An attractive feature of organometallic complexes as NLO materials is that molecular architectures can be easily modulated to optimize both the corresponding microscopic parameters, such as polarizability and hyperpolarizability, and the related macroscopic properties such as susceptibility and thermal stability [15].

Due to their centrosymmetric structures, nonsubstituted or symmetrically substituted organometallic complexes have been basically studied as third-order NLO materials [16]. Based on the structure and previous studies [2 – 7], one could expect that the title copper(II) complex (Fig. 1) may show third order NLO behavior. Theoretical calculations offer a quick and inexpensive way of predicting the NLO responses of the materials especially during the design phase of the new

0932–0776 / 06 / 1100–1355 $ 06.00

Table 1. Crystal and experimental data.

Compound	$C_{28}H_{22}Cu\,I_2N_2O_4$
Colour/shape	black/prismatic
Formula weight	767.82
Crystal system	monoclinic
Space group	$C2/c$
Unit cell dimensions [Å]	$a = 20.085(6)$
	$b = 9.806(7)$
	$c = 13.526(6)$
Volume [Å^3]	2657(2)
Z	4
Density (calculated) [gcm^{-3}]	1.92
Absorption coefficient [mm^{-1}]	3.2
$F(000)$	1484
Crystal size [mm^3]	$0.10 \times 0.25 \times 0.30$
θ Range for data collection [°]	2.03 – 29.99
Index ranges	$0 \le h \le 28$;
	$0 \le k \le 13$;
	$-19 \le l \le 18$
Independent reflections	3880
Reflections observed ($I \ge 2\sigma(I)$)	1755
Refinement method	Full-matrix least-squares on F^2
Data / parameters	3880 / 170
Goodness-of-fit on F^2	0.991
Final R indices [$I \ge 2\sigma(I)$]	$R = 0.0484$ $wR = 0.1261$
Final R indices (all data)	$R = 0.0604$ $wR = 0.1303$
(Δ/σ)max	0.001
Largest diff. peak and hole [eÅ^{-3}]	0.413 and −0.433

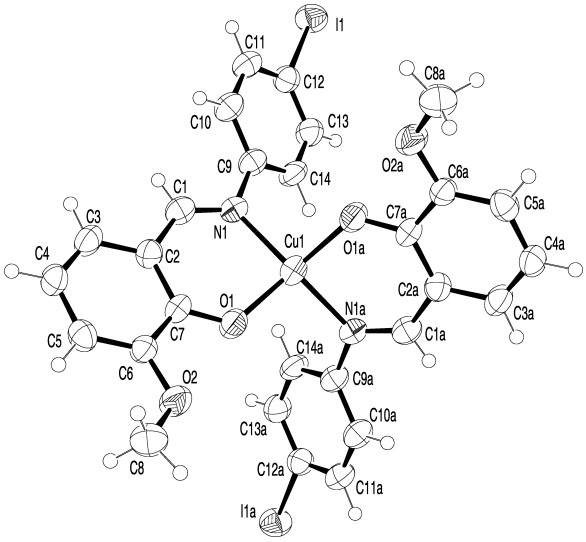

Fig. 1. The molecular structure of the Cu(II) complex. Atoms labeled with an "a" are related to their symmetry equivalents.

materials. Therefore, we have synthesized, characterized (UV-visible spectroscopy and X-ray structure determination) and theoretically evaluated the third order NLO response of the title Cu complex.

Table 2. Some selected bond lengths (Å) and angles (°) for the title complex.

I1-C12	2.110(7)	C7-C6	1.411(9)
Cu1-O1	1.907(5)	C10-C9	1.384(9)
O1-C7	1.310(8)	C10-C11	1.385(10)
N1-Cl	1.263(8)	C9-C14	1.380(10)
N1-C9	1.430(8)	O2-C6	1.360(8)
C2-C3	1.412(10)	O2-C8	1.409(9)
C2-C7	1.425(9)	C3-C4	1.343(10)
C2-C1	1.438(10)	C12-C11	1.375(10)
C7-O1	1.310(8)	C12-C13	1.380(9)
O1-Cu1- N1	98.1(2)	O1-Cu1- N1a	93.1(2)
N1-Cu1-N1a	149.5(3)	O1-Cu1-O1a	136.3(3)
C7-O1-Cu1	126.4(4)	C14-C9-N1	119.0(6)
C1-N1-C9	118.4(6)	C10-C9-N1	122.1(6)
C1-N1-Cu1	122.0(5)	N1-C1-C2	129.1(6)
C9-N1-Cu1	119.5(4)	C6-O2-C8	117.9(6)
C3-C2-C7	119.7(6)	C4-C3-C2	121.8(7)
C3-C2-C1	118.3(6)	C11-C12-C13	121.5(7)
C7-C2-C1	122.0(6)	C11-C12-I1	118.7(5)
O1-C7-C6	119.4(6)	C13-C12-I1	119.8(5)
O1-C7-C2	123.3(6)	C3-C4-C5	119.1(6)
C6-C7-C2	117.2(6)	C12-C11-C10	118.8(6)
C9-C10-C11	120.7(7)	O2-C6-C5	124.3(6)
C14-C9-C10	118.9(6)	O2-C6-C7	114.5(6)

Experimental Section

Reagents and techniques

2-Hydroxy-3-methoxy-benzaldehyde, 4-iodoaniline, copper(II) acetate, methanol and DMSO were purchased from Merck (Germany). Chloroform and *n*-hexane were purchased from Aldrich Chemical Co. The elemental analysis was performed on a LECO CHNS-932 C-, H-, N-analyzer. UV-visible absorption spectra were measured using a Perkin Elmer Lambda 2 series spectrophotometer. The UV-visible spectra of the compound in dimethylsulfoxide (DMSO), methanol, chloroform as polar solvents, and in *n*-hexane as a nonpolar solvent have been recorded by using the spectrophotometer in the range of 190 – 1100 nm, and are shown in Fig. 2. The maximum absorption wavelengths (λ) and molar extinction coefficients (ε) obtained from the UV-visible spectral analysis of the examined molecule in all the solvents are listed in Table 3.

Preparation of N-(2-hydroxy-3-methoxy-benzalidene)-4-iodoaniline and copper(II)bis{2-[(4-iodophenyl)imino-methyl]-6-methoxy-phenolate}

N-(2-Hydroxy-3-methoxybenzalidene)-4-iodoaniline was prepared by condensation of 2-hydroxy-3-methoxy-benzaldehyde (0.01 mol) and 4-iodoaniline (0.01 mol) in 100 mL of ethanol. The reaction mixture was stirred for 4 h and then placed in a freezer for 18 h. Suitable crystals were collected by filtration and then washed with cold ethanol. – $C_{14}H_{12}O_2NI$ (353.2): calcd. C 47.61, H 3.42,

Table 3. The maximum absorption wavelengths and molar extinction coefficients λ, nm (ε, $M^{-1}cm^{-1}$) respectively, obtained from the UV-visible spectral analysis of the Cu(II) complex in solvents of different polarity.

DMSO	Methanol	*n*-Hexane	Chloroform
403.3(1538)	403.3(2495)	400.0(789)	408.3(4510)
298.5(4256)	300.6(6478)	295.0(2768)	298.9(14652)
	226.6(10256)	214.7(29321)	
	201.2(18256)		

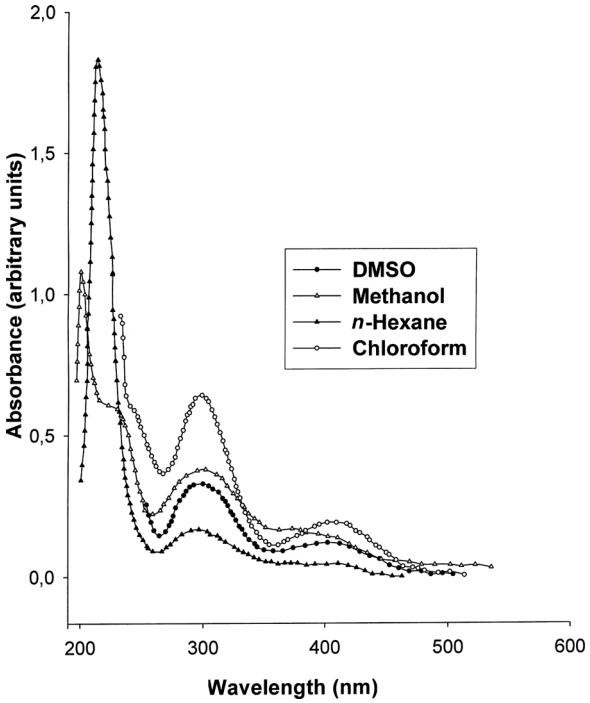

Fig. 2. UV-visible absorption spectra of the title compound in DMSO, chloroform, methanol and *n*-hexane.

N 3.97; found C 47.39, H 3.31, N 3.77. In order to obtain the copper(II)complex, $Cu(CH_3COO)_2 \cdot H_2O$ (0.01 mol) in methanol (50 mL) and N-(2-hydroxy-3-methoxybenzalidene)-4-iodoaniline (0.02 mol) in acetonitrile (100 mL) were mixed and heated at 335 K for 3 h. The solution was filtered and the filtrate was kept in a beaker at 283 K for crystallization. Black crystals started appearing after 2 – 3 d and were then collected by filtration. – $C_{28}H_{22}O_4I_2N_2Cu$ (767.8): calcd. C 43.80, H 2.89, N 3.65; found: C 43.26, H 2.47, N 3.45. Crystals suitable for X-ray diffraction were obtained by slow evaporation from a saturated ethanol solution.

X-ray structure determination

A crystal with dimensions of $0.10 \times 0.25 \times 0.30$ mm^3 was mounted on an Enraf-Nonius CAD-4 diffractometer employing graphite-monochromatized MoK_α radiation (λ = 0.71073 Å) [17]. Experimental conditions are summarized in Table 1. Cell parameters were determined by least-squares refinement on the setting angles of 25 reflections carefully centered on the diffractometer. Data reduction and corrections for absorption and crystal decomposition (1.2%) were carried out using the Stoe-REDU 4 Package [18]. The structure was solved by SHELXS-97 [19] and refined with SHELXL-97 [20]. The positions of H atoms bonded to C atoms were calculated (C-H distance 0.93 Å), and included in the structure factor calculation using a riding model. H atom displacement parameters were restricted to be $1.2U_{eq}$ of the parent atom. Bond lengths and bond angles are listed in Table 2. An ORTEP view of the molecular structure is given in Fig. 1 [21]. Crystallographic data (excluding structure factors) for the investigated structure have been deposited with the Cambridge Crystallographic Data Centre as supplementary publication number CCDC-290944 [22].

Theoretical calculations

In spite of the rapid development of highly advanced experimental techniques on NLO, the theoretical understanding of the NLO properties is also growing. There are many well-established and -tested computational codes to compute accurately the NLO properties of rather large molecular systems like organometallic complexes and polymers. Some of them are important as valuable theoretical tools used for computation of second hyperpolarizabilities (γ). The *ab initio* time-dependent Hartree-Fock (TDHF) method is most useful among the computational procedures [23]. Some important γ definitions in TDHF method are: $\gamma(0;0,0,0)$ and $\gamma(-3\omega;\omega,\omega,\omega)$. In these γ definitions, the first describes the static second hyperpolarizabilities at $\omega = 0$ frequency, and the second represents the dynamic hyperpolarizability at ω frequency for frequency tripling called the third-harmonic generation (THG) process.

In this paper, static second hyperpolarizabilities of the title Cu complex have been investigated employing an *ab initio* approach. We present a comprehensive theoretical study on the third-order NLO properties of the molecule using the TDHF method with a 3-21+G** polarized and diffused basis set. The TDHF procedure gives useful predictive values and can be of direct interest for understanding both static and dynamic first (β) and second hyperpolarizabilities (γ) of organic molecules and organometallic complexes. The γ values are very sensitive to the choice of the basis set

and the theoretical level of investigation. For a more precise determination of the second hyperpolarizabilities an extended basis set is required [24]. Both polarization and diffuse functions are required to accurately calculate the sensitive properties using Gaussian basis sets. Thus, the 3-21+G** basis set utilized in this study is probably rather adequate to compute the static second hyperpolarizabilities of the examined compound.

For the theoretical second hyperpolarizability calculations of the title Cu complex, the geometry was taken from the crystallographic data [22] as previously optimized at the *ab initio* closed-shell restricted Hartree-Fock level. The optimized structures were then used to calculate the static second hyperpolarizability tensor components with a 3-21+G** polarized and diffused basis set. To compute the static second hyperpolarizability values, we used the TDHF method implemented in the GAMESS program [25]. γ calculations were performed on a PC with an Intel Pentium IV operator, 512 MB RAM memory and 1.7 GHz frequency using the Linux PC GAMESS version running under Linux 7.3 environment.

In this study, the average static second hyperpolarizability values $\langle\gamma\rangle$ were calculated using the following expression [19]:

$$\langle\gamma\rangle = (1/5)\,[\gamma_{xxxx} + \gamma_{yyyy} + \gamma_{zzzz} + 2\,(\gamma_{xxyy} + \gamma_{xxzz} + \gamma_{yyzz})] \quad (1)$$

To calculate the static second hyperpolarizabilities, the origin of the Cartesian coordinate system $(x,y,z) = (0,0,0)$ has been chosen at the center of mass of the examined molecule in Fig. 1.

Results and Discussion

UV-visible spectroscopy

Electronic absorption spectra of the molecule in different solvents give us important pertinent information: Firstly, electronic absorption spectra give us the transparency region, which is very important for any possible NLO application [26–28]. The UV-visible spectrum (Fig. 2) shows that the title compound is transparent at wavelengths greater than 450 nm. Secondly, the electronic absorption spectra give information about the first hyperpolarizability of the molecule [29]: By substituting electron donor and electron acceptor groups, the intensity of the absorption band increases and the band shifts to longer wavelength (bathochromic behavior). This behavior is also seen when the polarity of the solvent is increased. It has been shown that the charge transfer absorption maximum shifts to longer wavelength on going from non-polar solvents to the most polar solvents. These solvent induced shifts of the absorption maxima (solvatochromic behavior) are generally considered as indicative of high molecular hyperpolarizability, β, and hence of potential bulk second order NLO properties. As it can be seen from Fig. 2 and Table 3, the complex shows little solvatochromic behavior indicating very weak second order NLO properties. This is expected because of the molecular symmetry of the title compound. Therefore, third order NLO properties were investigated in this paper.

On the other hand, the UV-visible absorption spectra of the complex exhibit two relatively intense bands. These two bands centered at 300 and 408 nm have been ascribed to $\pi \rightarrow \pi_1^*$ and $\pi \rightarrow \pi_2^*$ transitions, respectively. Albert *et al*. [30] have reached the conclusion that with the correct substitution of the push-pull system in the porphyrin ring, characterized by strong intramolecular $\pi \rightarrow \pi^*$ CT transitions, some specific electronic and structural properties of this system could produce high NLO responses.

Description of the crystal structure

The Cu atom lies on a two-fold axis and is coordinated by two O and two N atoms. Chelating Schiff base metal complexes may form *trans* and *cis* planar or tetrahedral structures. A strictly or slightly distorted planar *trans* configuration is characteristic for transition metal complexes of Cu^{II} with a CuN_2O_2 coordination sphere [31]. The Cu-N and Cu-O distances are 1.990(4) and 1.880(4) Å, respectively. The geometry around the metal centre can be described as distorted tetrahedral. The distortion from idealized geometry is due to the O1-Cu-N1 angle of 98.1(2)°, which is larger than the O1-Cu-N1a angle of 93.1(2)°. Discrete monomeric molecules are held together in the crystal by van der Waals interactions.

Computational results and discussion

NLO techniques are considered to be among the most structure-sensitive methods to study molecular structures and assemblies. Also, the incorporation of a heavy atom introduces more sublevels into the energy hierarchy as compared to organic molecules with the same number of skeletal atoms and this permits a

Table 4. All static $\gamma(0;0,0,0)$ components and $\langle\gamma\rangle(0;0,0,0)$ value [in atomic units] for the title molecule.

γ_{xxxx}	γ_{yyyy}	γ_{zzzz}	γ_{xxyy}	γ_{xxzz}	γ_{yyzz}	$\langle\gamma\rangle$
33229713.92	87560160.41	−190.84	6006970.57	−38057.64	−35632.39	26531248.91

greater number of allowed electronic transitions and hence enhances NLO effects. Since the potential of organic materials and metal complexes for NLO devices have been proven, NLO properties of many of these compounds have been investigated by both experimental and theoretical methods [32]. In the past five years, the efforts on NLO have been largely devoted to preparing third-order NLO materials using theoretical methods and exploring the structure-property relationships. Quantum chemical calculations have been shown to be useful in the description of the relationship between the electronic structure of the systems and its NLO response [33]. The computational approach allows the determination of molecular NLO properties as an inexpensive way to design molecules by analyzing their potential before synthesis and to determine high order hyperpolarizability tensors of molecules.

The calculated magnitudes of the static second hyperpolarizabilities for the title complex are reported in Table 4. As it is seen from this Table, the second hyperpolarizability of the title complex is non-zero since it is expected that the introduction of a donor (-OCH_3) /acceptor (-I) pair results in a larger polarization of the system in a way that increases significantly the $\langle\gamma\rangle$ nonlinear response. Organometallic complexes can also possess a large NLO response due to the attainment of low energy excited states with dipoles significantly different from the ground state dipole moment. The metal can have a large diversity of its coordination mode with various organic ligands affecting the nonlinear activity. The central metal atom in organometallic complexes can readily coordinate to conjugated ligands with π orbital overlap facilitating effective electronic communication and CT transitions leading to large dipole moment changes. The frontier molecular orbitals (MOs) in the Cu(II) complex consist of π orbitals having C=N and O_{2py} contributions, admixed to varying extents to metal *3d* orbitals of appropriate symmetry. In particular, the low energy CT feature may be characterized as principally $\pi \rightarrow \pi^*$ in character, essentially involving the metal $d_{xy} + 0_{2py}$ and the C=N orbitals, and is mainly responsible for the NLO response. As a result, $\langle\gamma\rangle$ values depend on a number of factors, which include the extent of π electron conjugation, the dimensionality of the molecules and the nature of substituents. Introduction of transition metals with partially filled *d*-shell is known to affect a number of CT mechanisms like MLCT, LMCT and *d*-*d* charge transfer [27].

Acknowledgements

This work was supported partly by Scientific and Technical Research Council of Turkey (TUBITAK) [105T132] and the Research Funds of Ankara University (CHE 2003 00 00 041), respectively.

[1] G. Rojo, G. de la Torre, J. García-Ruiz, I. Ledoux, T. Torres, J. Zyss, F. Agulló-López, Chem. Phys. **245**, 27 (1999).
[2] A. Karakaş, H. Ünver, A. Elmali, J. Mol. Struct. (Theochem) **712**, 117 (2004).
[3] A. Karakaş, A. Elmali, H. Ünver, I. Svoboda, Spectrochim. Acta: Part **A 61**, 2979 (2005).
[4] A. Karakaş, H. Ünver, A. Elmali, I. Svoboda, Z. Naturforsch. **60a**, 376 (2005).
[5] A. Elmali, A. Karakaş, H. Ünver, Chem. Phys. **309**, 251 (2005).
[6] H. Ünver, A. Karakaş, A. Elmali, T. N. Durlu, J. Mol. Struct. **737**, 131 (2005).
[7] H. Ünver, A. Karakaş, A. Elmali, J. Mol. Struct. **702**, 49 (2004).
[8] S. Shirk, R. G. S. Pong, F. J. Bartoli, A. W. Show, Appl. Phys. Lett. **63(14)**, 1880 (1993).
[9] A. Bhardwaj, P. O. Hedekvist, K. Vahala, J. Opt. Soc. Am. B **18 (5)**, 657 (2001).
[10] B. L. Davies, M. Samoc, Curr. Opin. Solid State Mater. Sci. **2**, 213 (1997).
[11] P. Romaniello, F. Lelj, J. Fluorine Chem. **125**, 145 (2004).
[12] L. T. Cheng, W. Tam, S. H. Stevenson, G. R. Meredith, G. Rikken, S. R. Marder, J. Phys. Chem. **95**, 10631 (1991).
[13] L. R. Dalton, A. W. Harper, R. Ghosn, W. H. Steier, M. Ziari, H. Fetterman, Y. Shi, R. V. Mustacich, A. K. Y. Jen, K. J. Shea, Chem. Mater. **7**, 1060 (1995).
[14] M. Blanchard-Desce, V. Alain, P. V. Bedworth, S. R. Marder, A. Fort, C. Runser, M. Barzoukas, S. Lebus, R. Wortmann, Chem. Eur. J. **3**, 1091 (1997).
[15] M. Spassova, V. Enchev, Chem. Phys. **298**, 29 (2004).
[16] J. S. Shirk, J. R. Lindle, F. J. Bartoli, C. A. Hoffman, Z. H. Kafafi, A. W. Snow, Appl. Phys. Lett. **55**, 1287 (1989).

[17] Molecular Structure Corporation. MSC/AFC Diffractometer Control Software, MSC 3200 Research Forest Drive, The Woodlands, TX 77381, USA (1994).
[18] Stoe-REDU, Stoe & Cie GmbH, Darmstadt, Germany (2001).
[19] G. M. Sheldrick, SHELXS-97, Program for the Solution of Crystal Structures, University of Göttingen, Germany (1997).
[20] G. M. Sheldrick, SHELXL-97, Program for the Refinement of Crystal Structures, University of Göttingen, Germany (1997).
[21] L. J. Farrugia, J. Appl. Crystallogr. **30**, 565 (1997).
[22] Further information may be obtained free of charge from The Cambridge Crystallographic Data Centre *via* www.ccdc.cam.ac.uk/data_request/cif.
[23] D. R. Kanis, M. A. Ratner, T. J. Marks, Chem. Rev. **94**, 195 (1994).
[24] J. L. Brédas, C. Adant, P. Tackx, A. Persoons, Chem. Rev. **94**, 243 (1994).
[25] Intel × 86 (win32, Linux, OS/2, DOS) version. PC GAMESS version 6.2, build number 2068. This version of GAMESS is described in: M. W. Schmidt, K. K. Baldridge, J. A. Boatz, S. T. Elbert, M. S. Gordon, J. H. Jensen, S. Koseki, N. Matsunaga, K. A. Nguyen, S. J. Su, T. L. Windus, M. Dupuis, J. A. Montgomery, J. Comput. Chem. **14**, 1347 (1993).
[26] S. Di Bella, I. Fragalá, Synthetic Metals **115**, 191 (2000).
[27] K. P. Unnikrishnan, J. Thomas, V. P. N. Nampoori, C. P. G. Vallabhan, Synthetic Metals **139**, 371 (2003).
[28] M. B. Nielsen, J.-P. Gisselbrecht, N. Thorup, S. P. Piotto, C. Boudon, M. Gross, Tetrahedron Letters **44**, 6721 (2003).
[29] M. Stahelin, D. M. Burland, J. E. Rice, Chem. Phys. Lett. **191**, 245 (1992).
[30] I. D. L. Albert, T. J. Marks, M. A. Ratner, Chem. Mater. **10**, 753 (1998).
[31] A. D. Garnovskii, A. L. Nivorozhkin, V. I. Minkin, Coord. Chem. Rev. **126**, 1 (1993).
[32] H. S. Nalwa, M. Hanack, G. Pawlowski, M. K. Engel, Chem. Phys. **245**, 17 (1999).
[33] a) P. Gunter, Nonlinear Optical Effects and Materials, Springer, Berlin, (2000); b) D. M. Burland, R. D. Miller, C. A. Walsh, Chem. Rev. **94**, 31 (1994).